FERMILAB-PUB-10-414-A

Dark Matter Annihilation in The Galactic Center As Seen by the Fermi Gamma Ray Space Telescope

Dan Hooper[1,2] and Lisa Goodenough[3]
[1] *Center for Particle Astrophysics, Fermi National Accelerator Laboratory, Batavia, IL 60510*
[2] *Department of Astronomy & Astrophysics, The University of Chicago, Chicago, IL 60637 and*
[3] *Center for Cosmology and Particle Physics, Department of Physics, New York University, New York, NY 10003*
(Dated: October 26, 2010)

We analyze the first two years of data from the Fermi Gamma Ray Space Telescope from the direction of the inner 10° around the Galactic Center with the intention of constraining, or finding evidence of, annihilating dark matter. We find that the morphology and spectrum of the emission between 1.25° and 10° from the Galactic Center is well described by a the processes of decaying pions produced in cosmic ray collisions with gas, and the inverse Compton scattering of cosmic ray electrons in both the disk and bulge of the Inner Galaxy, along with gamma rays from known points sources in the region. The observed spectrum and morphology of the emission within approximately 1.25° (~ 175 parsecs) of the Galactic Center, in contrast, cannot be accounted for by these processes or known sources. We find that an additional component of gamma ray emission is clearly present which is highly concentrated around the Galactic Center, but is not point-like in nature. The observed morphology of this component is consistent with that predicted from annihilating dark matter with a cusped (and possibly adiabatically contracted) halo distribution ($\rho \propto r^{-1.34\pm0.04}$). The observed spectrum of this component, which peaks at energies between 2-4 GeV (in E^2 units), is well fit by that predicted for a 7.3-9.2 GeV dark matter particle annihilating primarily to tau leptons with a cross section in the range of $\langle \sigma v \rangle = 3.3 \times 10^{-27}$ to 1.5×10^{-26} cm^3/s, depending on how the dark matter distribution is normalized. We discuss other possible sources for this component, but argue that they are unlikely to account for the observed emission.

PACS numbers: 95.35.+d; 95.85.Pw

I. INTRODUCTION

The inner volume of the Milky Way is one of the most promising targets for the indirect detection of dark matter. In particular, due to the high densities of dark matter predicted to be present in the region, the innermost tens or hundreds of parsecs of our galaxy is generally expected to produce the single brightest source of dark matter annihilation products, including gamma rays [1].

Since its launch in June of 2008, the Large Area Telescope (LAT) onboard the Fermi Gamma Ray Space Telescope (FGST) has been observing gamma rays in the range of approximately 300 MeV to 100 GeV over the entire sky, including from the direction of the Galactic Center. Data from the FGST has been used to search for dark matter annihilations taking place in dwarf spheroidal galaxies [2], galaxy clusters [3], over cosmological volumes [4], throughout the Galactic Halo [5], in dark matter subhalos [6], and in the Galactic Center [7]. In this article, we revisit the Galactic Center region as observed by the FGST and perform a detailed study of the spectral and morphological features of these gamma rays with the intention of either placing constraints on, or finding evidence for, dark matter annihilations taking place. In the course of this study, we found compelling evidence for a component of emission that is highly concentrated in the inner degree around the Galactic Center, and which is spectrally and morphologically distinct from all known backgrounds. This excess component, however, is very consistent with the spectrum and angular distribution predicted from annihilating dark matter in a cusped, and possibly adiabatically contracted, halo profile ($\rho \propto r^{-1.34\pm0.04}$), with a mass of 7.3-9.2 GeV, and annihilating primarily to tau leptons. The normalization of the observed component requires the dark matter annihilation cross section to fall within the range of $\langle \sigma v \rangle = 3.3 \times 10^{-27}$ to 1.5×10^{-26} cm^3/s, similar to that required of dark matter in the form of a simple thermal relic.

The remainder of this paper is structured as follows. In the following section, we discuss the process of dark matter annihilation and the calculation of the angular distribution and spectrum of gamma ray annihilation products from the Galactic Center. In Sec. III, we study the gamma ray emission as observed by the FGST in the inner 2-10° around the Galactic Center, and find it to be well described by pion decay and inverse Compton scattering in the disk and bulge of the Inner Galaxy, in addition to containing emission from known point sources. In Sec. IV, we study in the inner 2° and identify a component of emission that is distinct from known backgrounds and point sources, and that is highly concentrated around the Galactic Center, but not point-like in nature. In Sec. V, we discuss this component within the context of annihilating dark matter. In Sec. VI, we discuss other possibilities for the origin of this component, such as unresolved point sources or the decays of energetic pions, but argue that these are unlikely to account for the observed emission. In Sec. VII, we compare the results of this study to those presented in our

previous work [7]. Finally, in Sec. VIII, we discuss some of the implications of these results and draw our conclusions.

II. GAMMA RAYS FROM DARK MATTER ANNIHILATIONS NEAR THE GALACTIC CENTER

Dark matter halos are most dense at their centers. If the dark matter consists of particles that can self-annihilate, the innermost volume of the Milky Way's halo potentially may produce an observable flux of dark matter annihilation products, including gamma rays. The energy and angular dependent flux of such gamma rays is described by

$$\Phi_\gamma(E_\gamma,\psi) = \frac{\mathrm{d}N_\gamma}{\mathrm{d}E_\gamma}\frac{\langle\sigma v\rangle}{8\pi m_X^2}\int_{\rm los}\rho^2(r)\mathrm{d}l, \tag{1}$$

where $\langle\sigma v\rangle$ is the dark matter annihilation cross section multiplied by the relative velocity of the two dark matter particles (averaged over the velocity distribution), m_X is the mass of the dark matter, ψ is the angle observed relative to the direction of the Galactic Center, $\rho(r)$ is the dark matter density as a function of distance to the Galactic Center, and the integral is performed over the line-of-sight. $\mathrm{d}N_\gamma/\mathrm{d}E_\gamma$ is the gamma ray spectrum generated per annihilation, which depends on the mass and dominant annihilation channels of the dark matter particle.

It is convenient to rewrite this equation as

$$\Phi_\gamma(E_\gamma,\psi) \approx 2.8\times10^{-10}\,\mathrm{cm^{-2}\,s^{-1}\,sr^{-1}}\times\frac{dN_\gamma}{dE_\gamma}\left(\frac{\langle\sigma v\rangle}{3\times10^{-26}\,\mathrm{cm^3/s}}\right)\left(\frac{100\,\mathrm{GeV}}{m_{\rm X}}\right)^2 J(\psi) \tag{2}$$

where the dimensionless function $J(\psi)$ depends only on the dark matter distribution and is defined by convention as

$$J(\psi) = \frac{1}{8.5\,\mathrm{kpc}}\left(\frac{1}{0.3\,\mathrm{GeV/cm^3}}\right)^2\int_{\rm los}\rho^2(r(l,\psi))\mathrm{d}l\,. \tag{3}$$

To calculate $J(\psi)$, a model for the dark matter halo distribution must be adopted. A commonly used parametrization of halo profiles is given by

$$\rho(r) = \frac{\rho_0}{(r/R)^\gamma[1+(r/R)^\alpha]^{(\beta-\gamma)/\alpha}}\,, \tag{4}$$

where $R\sim$ 20-30 kpc is the scale radius of the halo and ρ_0 normalizes the halo's total mass. Among the most frequently used models is the Navarro-Frenk-White (NFW) profile, which is described by $\alpha=1$, $\beta=3$ and $\gamma=1$ [8]. When considering the region of the Galactic Center, the most important feature of the halo profile is the inner slope, γ. In the inner parsecs of our galaxy, in which we are most interested, there are reasons to expect this slope to become steeper than described by NFW. In particular, the gravitational potential in the inner Milky Way is dominated by baryons rather than dark matter, which are not included in N-body simulations. Although the precise impact of baryons on the dark matter distribution is difficult to predict, an enhancement of the inner slope due to adiabatic contraction is generally expected [9].

The remaining factors in Eq. (2) depend on the properties of the dark matter particle, including its mass, annihilation cross section, and dominant annihilation channels. A reasonable benchmark value for the annihilation cross section is $\langle\sigma v\rangle\approx3\times10^{-26}\,\mathrm{cm^3/s}$, which for a simple thermal relic will yield a density of dark matter that is similar to the cosmologically measured abundance [10]. If dark matter annihilations in the early universe take place largely through P-wave processes, resonant processes, or co-annihilations, then smaller values of $\langle\sigma v\rangle$ are possible.

The challenge in identifying gamma rays from dark matter annihilations is not in merely observing the signal. A 50 GeV dark matter particle, for example, with $\langle\sigma v\rangle\approx3\times10^{-26}\,\mathrm{cm^3/s}$, and distributed according to NFW, should lead to the detection by the FGST of on the order of hundreds of gamma rays per year from dark matter in the inner degree of our galaxy. In order to make use of this signal, however, it must be distinguished from the various astrophysical backgrounds present in the Inner Galaxy [11]. Fortunately, the products of dark matter annihilations are predicted to possess distinctive characteristics that can be used to accomplish this. In particular, by searching for a highly concentrated signal around the Inner Galaxy (more centrally concentrated than diffuse astrophysical mechanisms, but more extended than a single point source), with the spectral shape consistent with that predicted from dark matter annihilations, it may be possible to identify a component of gamma rays originating from dark matter. In the following sections of this paper, we attempt to do this, by first turning our attention to the astrophysical gamma ray backgrounds in the region of the inner Milky Way.

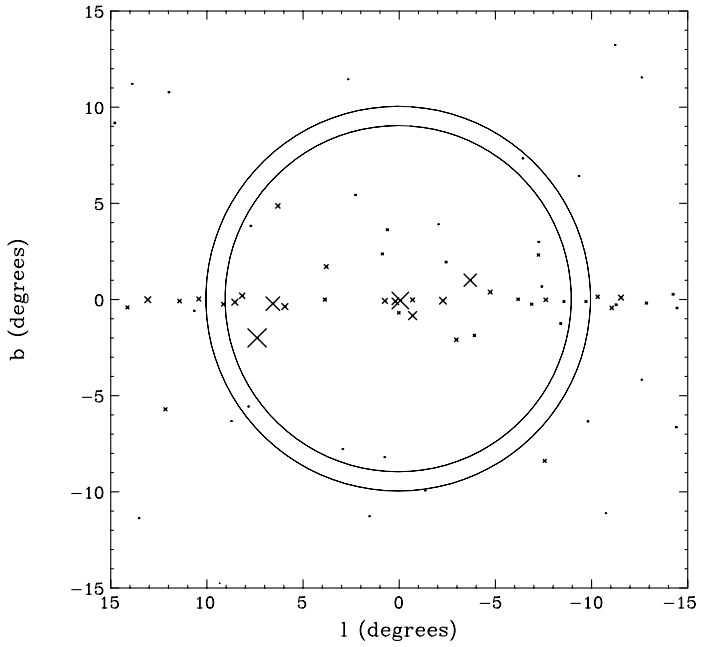

FIG. 1: The locations of the 69 known point sources included in our study. The size of each X is proportional to the intensity of that source in the range of 1-100 GeV, as described in the Fermi First Source Catalog. The region between the two solid circles is that shown in Figs. 2-5.

III. MODELING THE BACKGROUNDS OF THE INNER GALAXY

We begin by modeling the emission from the region of the Galactic Center with three distinct components:

- Emission from the Disk – We model this component with a gaussian width around $b = 0$, with the width, intensity, and spectral shape fit to the data. The width, intensity, and spectral shape of this component is allowed to vary freely with galactic longitude, l, although we find that these parameters do not significantly vary along the disk.

- Emission distributed with spherical symmetry about the Galactic Center – We model this component to have intensity and spectral shape that is constant with direction from the Galactic Center, but that can vary freely with distance to the Galactic Center.[1] It is in this component that any contribution from dark matter annihilation would be expected to appear. Astrophysical contributions, such as those from processes taking place throughout the Galactic Bulge, also appear in this component.

- Emission from known point sources – We include the 69 sources in the Fermi First Source Catalog [13] with coordinates in the range of $l = (-15°, 15°)$ and $b = (-15°, 15°)$. We show the locations of these sources in Fig. 1, where the size of each X is proportional to the intensity of the source over the energy range of 1-100 GeV.

For a given set of model parameters (disk widths, spectral shapes, etc.), we convolve the emission with the the FGST's LAT point spread function (PSF), which describes the accuracy with which the arrival direction of a gamma ray can be determined. For front-converting (thin) events (due to their inferior PSF, we do not consider back-converting events in this study), we model FGST's PSF according to

$$\mathcal{P}(E_\gamma, \theta) = \sqrt{\frac{2}{\pi}} \exp\left[- \frac{\theta^2 C^2}{2\, P_{68}^2(E_\gamma)} \right], \tag{5}$$

[1] Here and elsewhere throughout this study, the distance to the Galactic Center refers to distance to the dynamical center, which we take to be $b = 0.0442°$, $l = -0.055°$ [12], rather than $b = 0$, $l = 0$.

where θ is the difference between the measured and actual directions of the observed gamma ray. The function P_{68} is the angle within which 68% of the gamma rays are reconstructed, and is well fit (in degrees) by

$$\begin{aligned} \log_{10}[P_{68}(E_\gamma)] &= -0.276 - 0.674 \log_{10}[E_\gamma/1\,\mathrm{GeV}], \qquad E_\gamma < 20\,\mathrm{GeV} \\ \log_{10}[P_{68}(E_\gamma)] &= -0.785 - 0.283 \log_{10}[E_\gamma/1\,\mathrm{GeV}], \qquad E_\gamma > 20\,\mathrm{GeV}. \end{aligned} \tag{6}$$

The quantity C appearing in Eq. 5 accounts for the non-gaussianity of the LAT's PSF. We fit this according to [14]

$$\begin{aligned} C &= 1, \qquad \theta < P_{68} \\ C &= 0.735 + 0.265 \left(\frac{P_{68}}{\theta} \right), \qquad \theta > P_{68}. \end{aligned} \tag{7}$$

At angular distances of more than 1-2° from the Galactic Center, the disk component of the emission can be clearly and easily separated from the other components. For this reason, we begin by studying only the region of the sky with $\sqrt{l^2 + b^2} > 2°$. For a given angular annulus, we fit the data to a combination of the three components described above, and consider one energy bin at a time (distributed logarithmically in energy, with ten bins per decade). For each combination of energy and distance from the Galactic Center, we find the combination of the following parameters that yields the best overall chi-square fit: the intensity of the disk emission for $l < 0°$, the intensity of the disk emission for $l > 0°$, the width of the disk emission for $l < 0°$, the width of the disk emission for $l > 0°$, and the intensity of the spherically symmetric emission. For simplicity, we fix the intensity of each point source assuming that it has a power-law spectrum with an index and intensity as described in the Fermi First Source Catalog (the central values that are quoted). At times, this simplifying choice will not be supported by the data (departures from power-law behavior are evident for some of the point sources), but this impacts our overall results only slightly.

In Figs. 2-5, we show the angular distribution (meaning with the direction from the Galactic Center) of the (front converting) events observed by FGST between 9 and 10 degrees away from the Galactic Center in the first 16 energy bins (300 MeV to 11.94 GeV), and compare this to that predicted for our best-fit model parameters. In each frame, the emission from the disk is clearly apparent and in some cases emission from individual point sources can be seen (compare to the point sources between the two circles shown in Fig. 1). The data shown corresponds to that collected between August 4, 2008 and August 12, 2010.

The most significant discrepancies between our best fit model and the data, as shown in Figs. 2-5 (and also over other angular ranges), results from our simplistic treatment of point sources. Because we have not allowed the intensity of the point source contributions to float in this fit, but rather have fixed them to the overall flux and power-law spectral index listed in the FGST First Source Catalog, there are evident examples in which either brighter or dimmer point source emission would provide a better fit, relative to that included in our simple model. Notice, for example, the E_γ =599-754 MeV and 754-949 MeV frames of Figs. 3-4, at approximately $\arctan(b/l) \approx 220 - 230°$. Here the spectrum of the responsible nearby point source (clearly identifiable in Fig. 1 as 1FGL J1802.5-3939, located at $l = -7.5581°$, $b = -8.3935°$) evidently exceeds that predicted by the best fit power-law. If it were not for considerations of computation time, we could fit for the individual intensities of each point source in each energy bin. Given that less than 7% of the total gamma ray flux in the inner ±15° window is associated with resolved point sources, this choices does not significantly impact our extraction of the spectral shapes or intensities of the gamma ray emission from the disk or from the spherically symmetric components.

We have repeated this procedure to derive the spectra of the disk and spherically symmetric components of the gamma ray emission over various regions of the Inner Galaxy (between 2° and 10° from the Galactic Center). The results are shown in Figs. 6-8. We find that the emission from the disk has a fairly uniform spectral shape and overall intensity, varying only slightly along the disk (with l). The spherically symmetric emission also shows no discernible variation in the spectral shape, but does become steadily brighter as we move closer to the Galactic Center.

The spectra shown in Figs. 6-8 can be easily accounted for with known emission mechanisms. In particular, their spectral shapes are consistent with being dominated by gamma rays from neutral pion decay, with a smaller but not insignificant contribution from inverse Compton scattering (a small contribution from Bremsstrahlung may also be present). In Fig. 9, we show the shapes of the spectra predicted from these emission mechanisms, as calculated using the publicly available code GALPROP [15]. The solid lines shown in Figs. 6-7 correspond to the predicted spectrum from pion decay and inverse Compton scattering, with relative normalizations as shown in Fig. 9. This provides a good overall fit to the observed spectra from the disk. In Fig. 8, the solid line again represents the contribution from pion decay and inverse Compton scattering, but with a larger fraction of the emission from inverse Compton scattering (7.15 times larger, relative to the pion component, than in the disk). Again, this provides a good overall fit to the observed spectra. The greater relative contribution from inverse Compton scattering (or equivalently, the lesser relative contribution from pion decay) is likely the consequence of lower gas densities away from the Galactic Disk.

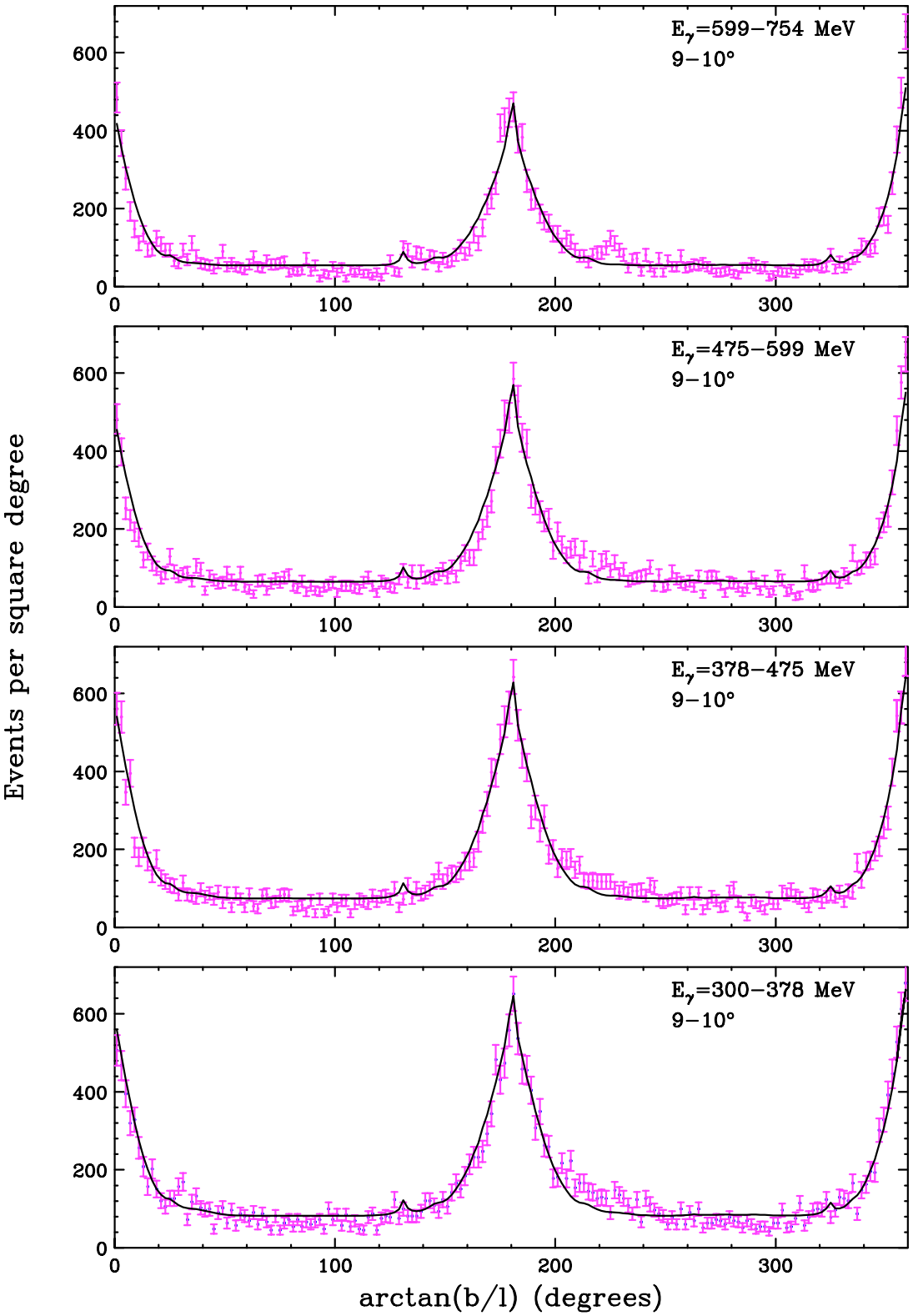

FIG. 2: The best fit model for the emission in the four lowest energy bins from the region between 9 and 10 degrees from the Galactic Center (the region between the two circles shown in Fig. 1), compared to the observations of the FGST. See text for details.

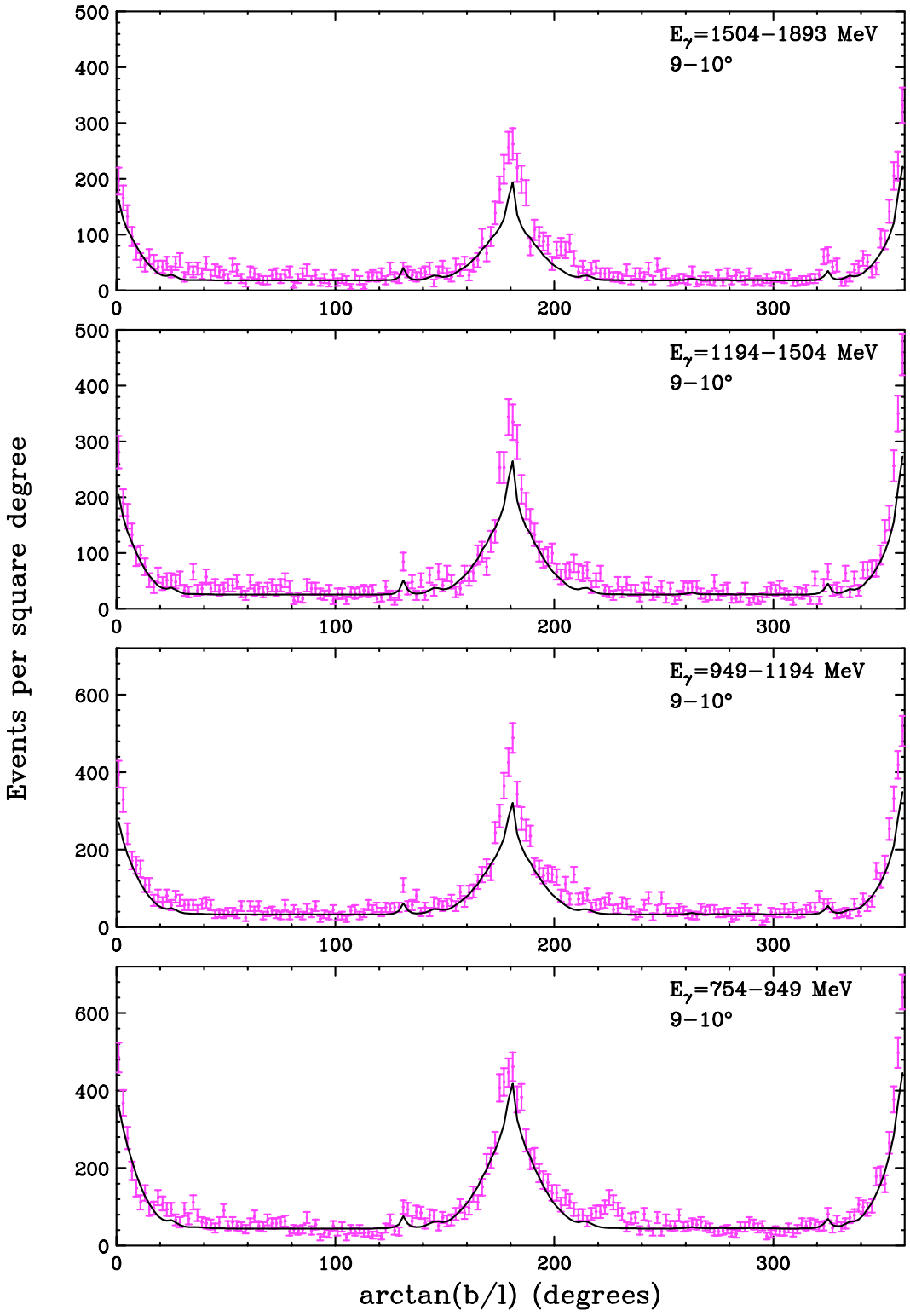

FIG. 3: The same as Fig. 2, but for higher energy bins, as labeled.

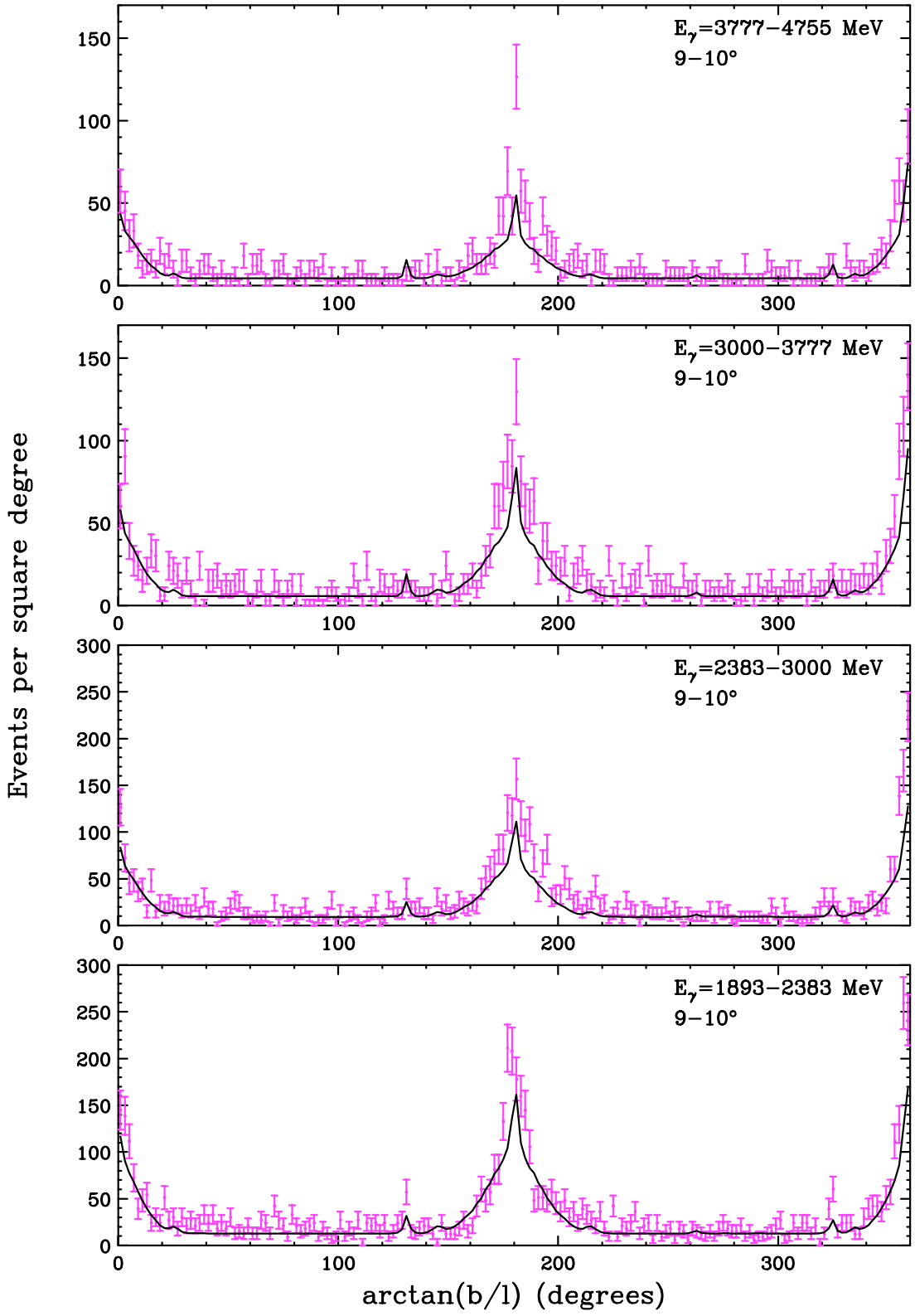

FIG. 4: The same as Fig. 2, but for higher energy bins, as labeled.

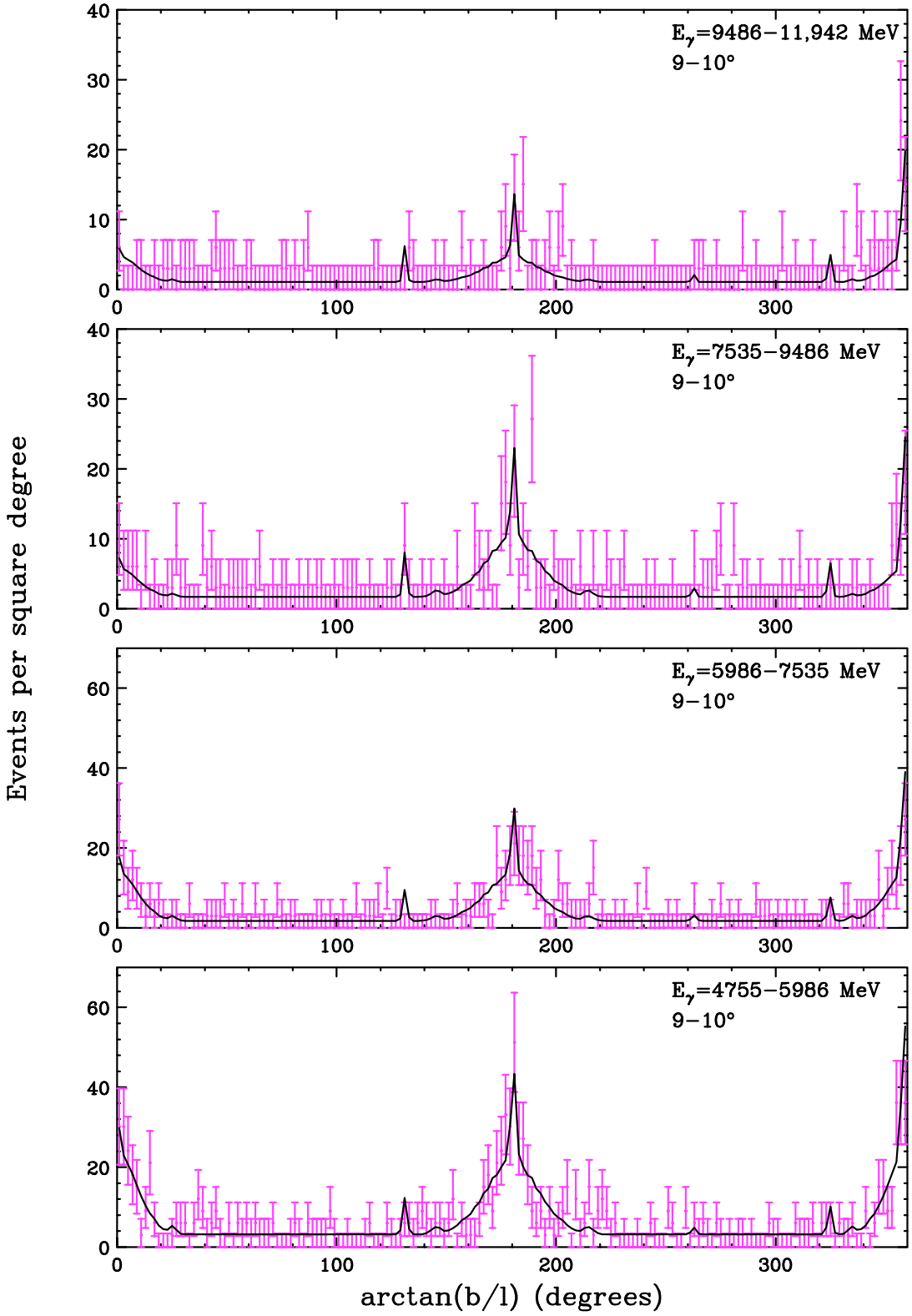

FIG. 5: The same as Fig. 2, but for higher energy bins, as labeled.

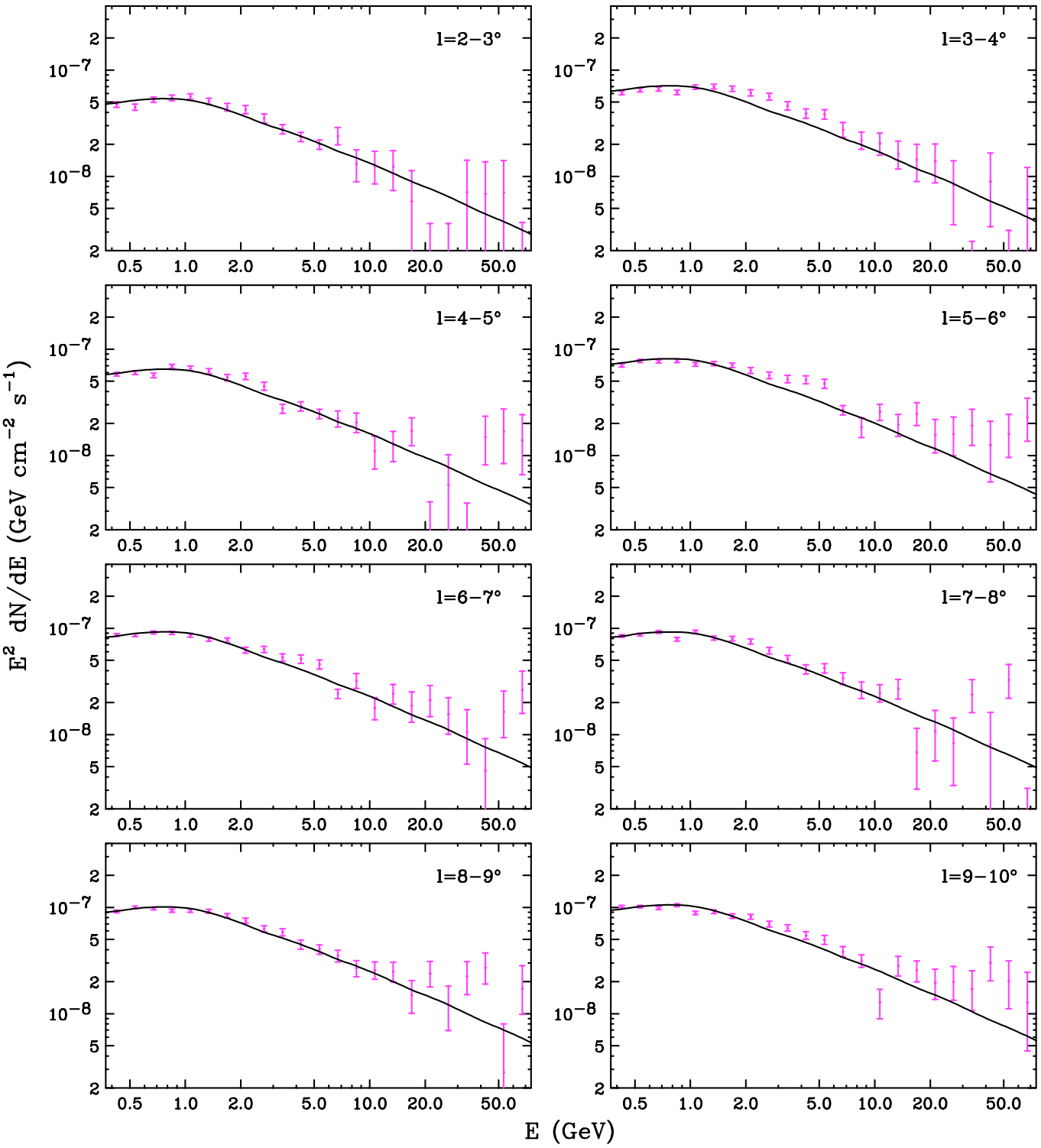

FIG. 6: The spectrum of emission from the disk for $l > 2°$. Note that the spectral shape and intensity varies only slightly along the plane. The solid line is the shape predicted from the combination of pion decay and inverse Compton scattering (a small contribution from Bremsstrahlung may also be present), as shown in Fig. 9. The overall normalization of this emission varies by less than a factor of 2 among the frames. See text for details.

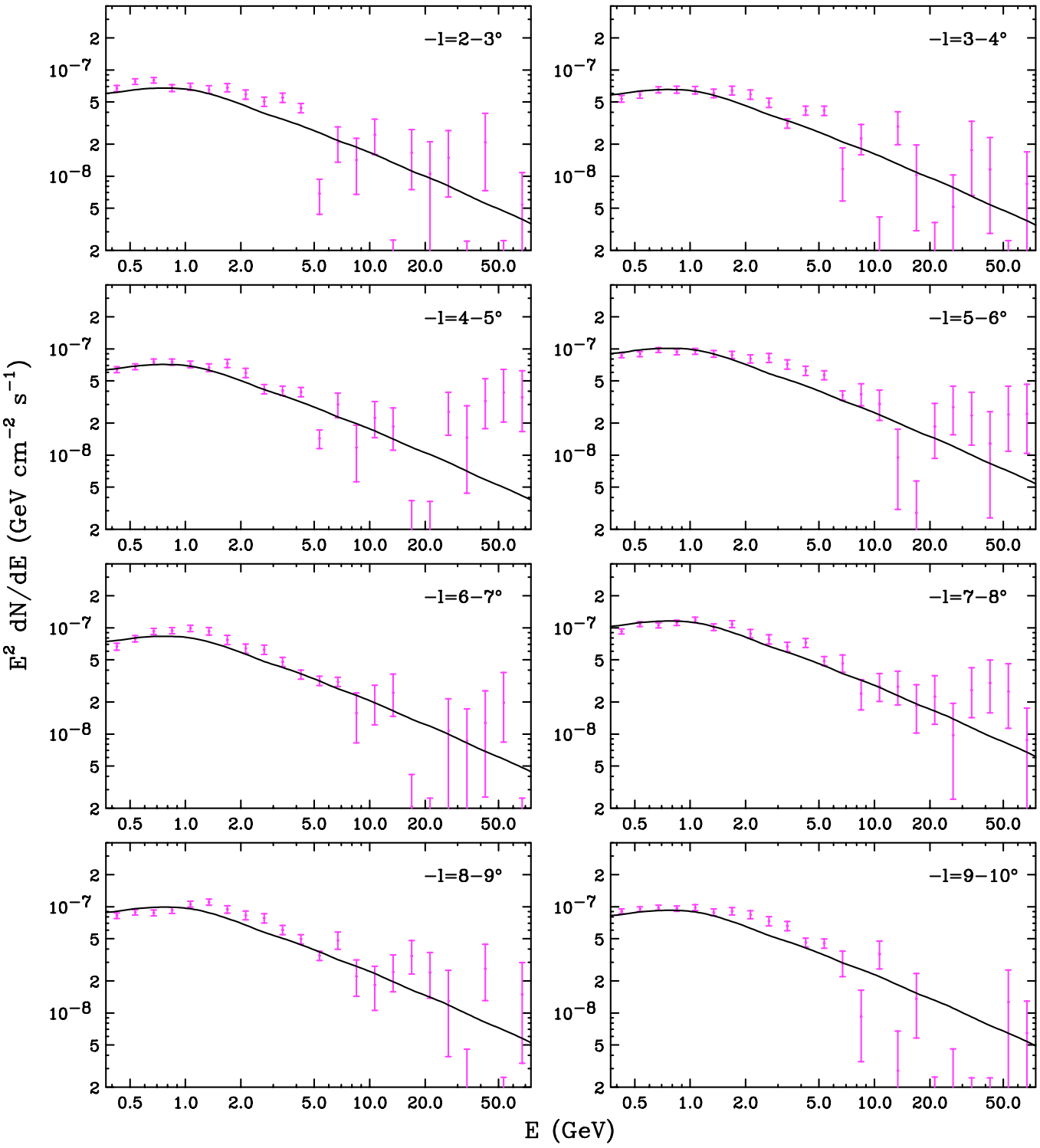

FIG. 7: The spectrum of emission from the disk for $l < -2^\circ$. Note that the spectral shape and intensity varies only slightly along the plane. The solid line is the shape predicted from the combination of pion decay and inverse Compton scattering (a small contribution from Bremsstrahlung may also be present), as shown in Fig. 9. The overall normalization of this emission varies by less than a factor of 2 among the frames. See text for details.

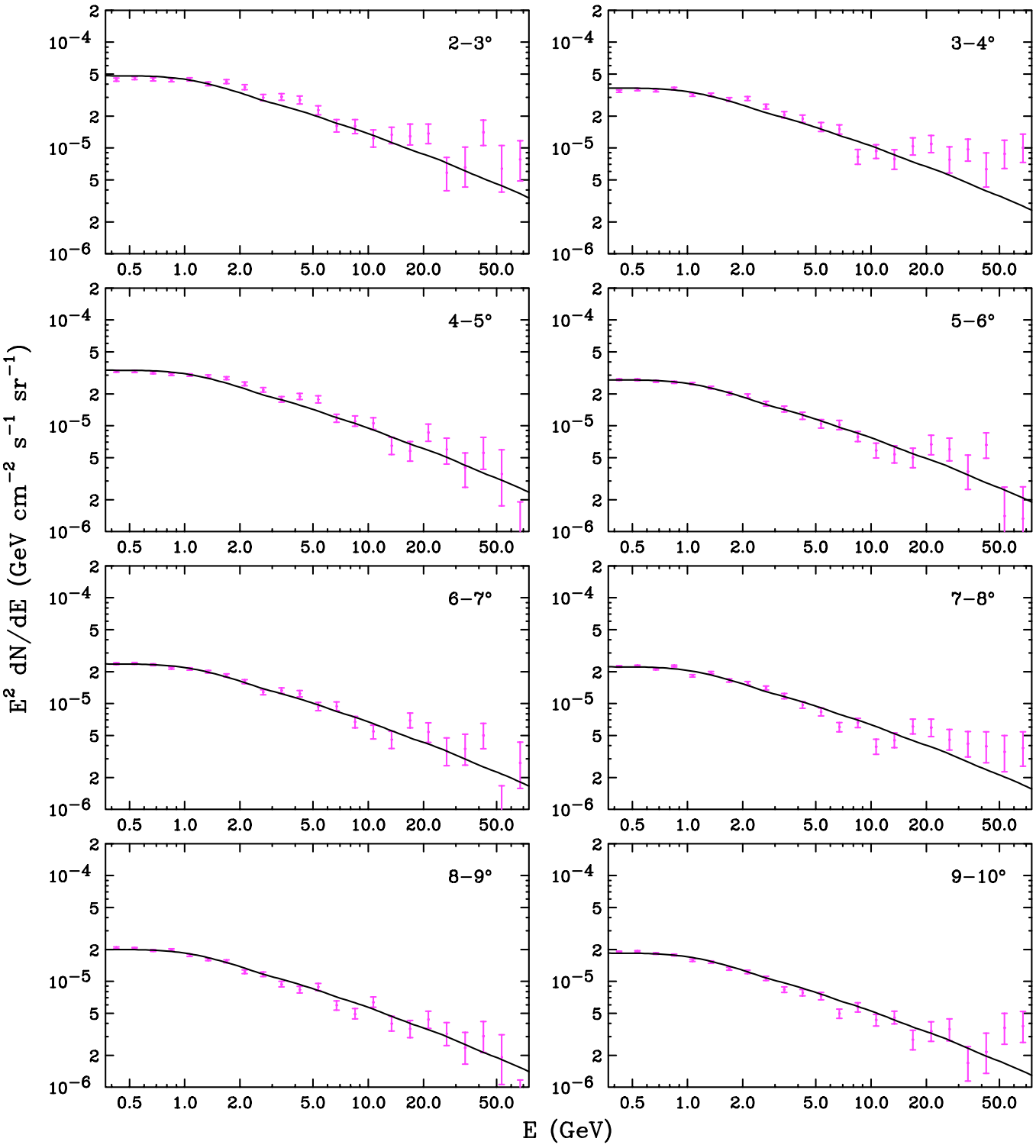

FIG. 8: The spectrum of the emission that is distributed with spherical symmetry around the Galactic Center (not disk-like or associated with known point sources), for different ranges of angles from the Galactic Center (each frame shows the emission from a given angular annulus). Although the spectral shape does not discernibly change with distance to the Galactic Center, the overall intensity does vary, becoming brighter closer to the Inner Galaxy. The solid line is the shape predicted from the combination of pion decay and inverse Compton scattering (a small contribution from Bremsstrahlung could also be present), as shown in Fig. 9, but with a larger relative flux of inverse Compton gamma rays than in Figs. 6-7 (the spectral shape of the bulge emission contains somewhat more high energy emission than that from the disk).

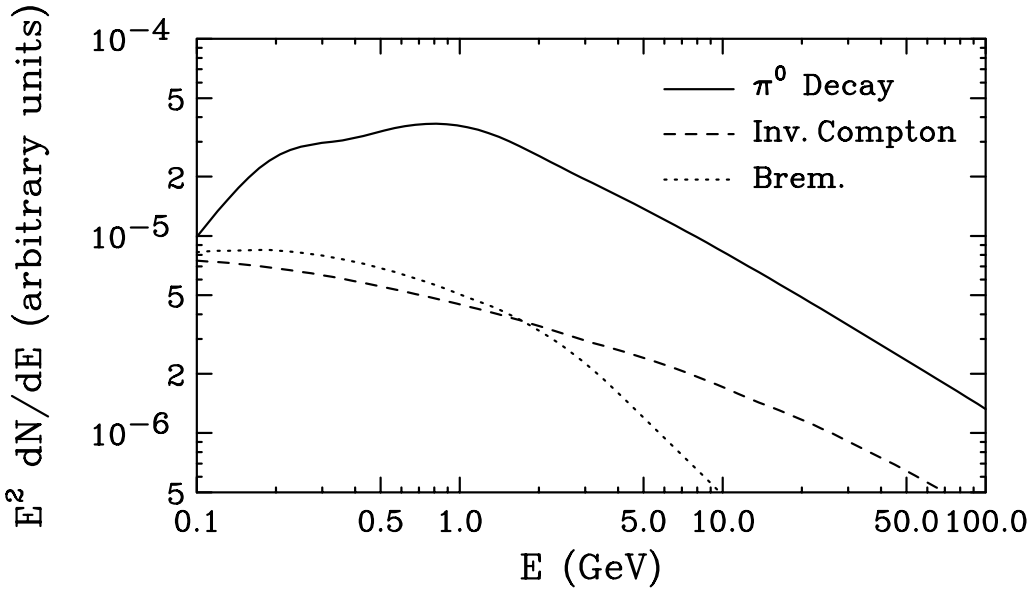

FIG. 9: The predicted spectral shapes of gamma rays from pion decay, inverse Compton scattering, and Bremsstrahlung in the region around the Galactic Center, as generated using the publicly available code GALPROP [15].

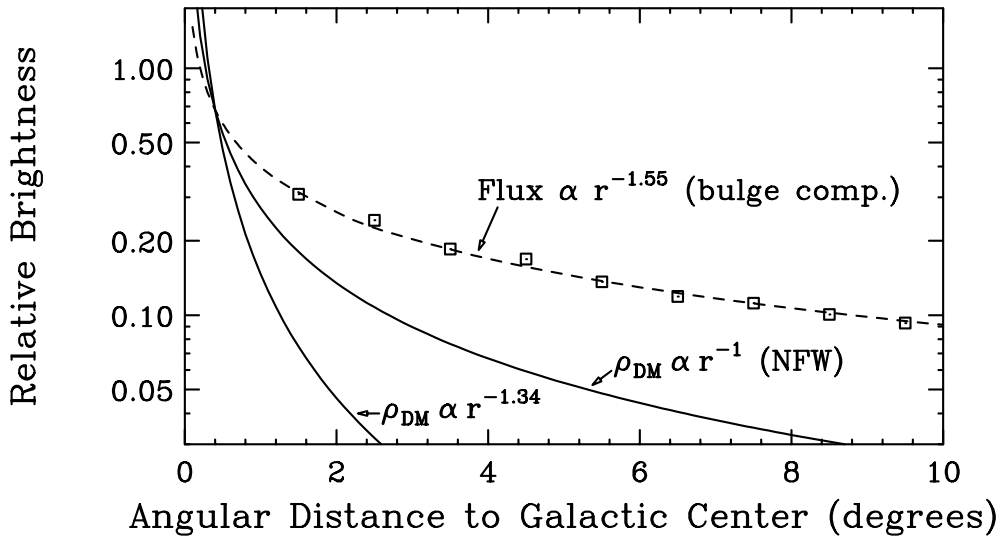

FIG. 10: The relative brightness, integrated along the line-of-sight, of the emission that is distributed with spherical symmetry around the Galactic Center (*ie.* the bulge component), as a function of the distance to the Galactic Center (squares), compared to that predicted for emission that is distributed as $r^{-1.55}$, where r is the distance to the Galactic Center (dashed line). For comparison, we also show the distribution for emission from dark matter annihilations using a NFW ($\gamma = 1$) halo profile or a NFW-like profile with $\gamma = 1.34$ (solid).

The variation of the intensity of the observed disk emission with distance from the Galactic Center is well described by a density profile of emission which scales with $r^{-1.55}$ within the inner 2 kiloparsecs or so, where r is the distance to the Galactic Center (see Fig. 10). This component is likely associated primarily with gas in the Galactic Bulge. Given the agreement of the observed spectrum with that predicted from pion decay and inverse Compton scattering, we see no evidence of any exotic component among the bulge emission (outside of 2° from the Galactic Center).

IV. THE INNER TWO DEGREES AROUND THE GALACTIC CENTER

Within 1-2° of the Galactic Center, it is more difficult to clearly separate the spherically symmetric contributions from those originating from the disk. Instead, we compare in Fig. 11 the total emission in the innermost angular regions to a model consisting of the extrapolated disk emission (which was found to be relatively constant between $|l| = 2 - 10°$) and bulge emission increasing with angle according to the best fit $r^{-1.55}$ profile. In each frame, the dotted and dashed lines represent the bulge and disk components of our model, respectively, while the solid line denotes the sum of these components. For regions more than approximately 1.25° away from the Galactic Center, this model describes the total observed spectra very well. Inside of this radius, however, the spectral shape changes considerably, becoming considerably more intense over the range of about 1-5 GeV. No combination of the spectra from the mechanisms shown in Fig. 9 can account for this transition.

To further elucidate this observed transition in the inner ∼1.25° of our Galaxy, we plot in Figs. 12-13 the angular profile of the observed emission in 16 energy bins. Again, the dotted, dashed and solid lines denote the bulge, disk and bulge+disk components, respectively. In each energy bin, the model describes the observed profile beyond 1.25° quite well. In the innermost regions of the Galaxy, however, a clear excess of emission between about 600 MeV and 6 GeV is present.

For each energy bin, we do a fit to the angular profile (as shown in Fig. 12-13), for a combination of disk and bulge components as shown, plus each point source in the Fermi First Source Catalog, and a additional spherically symmetric component with a profile of emission proportional to $r^{-2\gamma}$, where γ is treated as a free parameter (if associated with dark matter annihilation, this parameter γ is the same γ that defines the inner slope of the dark matter profile). In calculating the quality of the fits, we include a small 3% systematic error, which is intended to account for the spatial variation in the disk and bulge emission from, for example, unresolved point sources. Assuming that γ does not vary from energy bin to energy bin, we find that we are able to constrain the profile of the additional component to $\gamma = 1.34 \pm 0.04$, at the 90% confidence level. We then use our fit to extract the spectrum of the bright point source located at the Galaxy's dynamical center Center (see Fig. 14) and of the additional spherically symmetric component (Fig. 15). Although the inclusion of the other nearby (and more faint) point sources does slightly improve the quality of the fit to the data, the spectra of these sources cannot be extracted with much detail.

The extracted spectrum of the Galactic Center point source is consistent with a power-law above ∼1 GeV, and even agrees very well with the extrapolation of the spectrum at higher energies, as measured by the HESS [12] and other ground based gamma ray telescopes [16]. In Fig. 14, we show as a solid line the power-law spectrum as extrapolated from HESS. The spectrum of this sources falls off below ∼1 GeV; a feature that can also be clearly seen in Fig. 12.

In Fig. 15, we show the spectrum of the excess emission within 1° of the Milky Way's dynamical center. By excess emission, we mean the emission that is not accounted for by the disk and bulge components, and that not associated with any known point sources. The excess emission is clearly distinct from these other components, both morphologically (highly concentrated within the inner one degree) and spectrally (peaking at higher energies than the astrophysical backgrounds, such as those from pion decays). In this figure, we also compare the spectrum of the excess emission to that predicted from dark matter annihilations. We find a particularly good fit for dark matter particles with masses in the range of 7.3-9.2 GeV annihilating to $\tau^+\tau^-$, as shown by a solid line in the figure. We also show results for a somewhat heavier dark matter particle ($m = 30$ GeV) which annihilates to either bottom or charm quarks. These cases predict a somewhat broader spectral peak, however, and do not provide a fit consistent with the spectrum observed. An ~ 8 GeV particle which annihilates primarily to tau leptons may annihilate to $b\bar{b}$ or $c\bar{c}$ final states up to 10-20% of the time, however, without negatively impacting the overall quality of the fit.

V. ANNIHILATING DARK MATTER

In this section, we discuss the properties of the dark matter that are required to accommodate the excess gamma ray emission described in the prior section. As previously stated, good fits are found for dark matter masses in the range of 7.3 to 9.2 GeV, and which annihilate primarily to a $\tau^+\tau^-$ final state (in addition to any annihilations to final states which do not yield large fluxes of gamma rays, such as e^+e^-, $\mu^+\mu^-$, $\nu\bar{\nu}$, etc.). Up to 10-20% of annihilations could also proceed to $b\bar{b}$ or $c\bar{c}$ final states.

The value of the dark matter's annihilation cross section required to normalize the gamma ray spectrum to that shown in Fig. 15 depends somewhat on how the distribution dark matter in the Inner Galaxy is itself normalized. The somewhat steep inner slope of the profile ($\gamma = 1.34 \pm 0.04$) that is inferred from the data may be the result of adiabatic contraction [9] occurring in the inner kiloparsecs of the Milky Way. If this is the case, then the profile's slope may be shallower ($\gamma \sim 1$) farther away the Galactic Center, for example.

If we simply assume that the slope of 1.34 continues to at least the Solar Circle ($r \approx 8$ kpc), we find a value of J (see Eqs. 2-3) averaged over a radius of 1° around the Galactic Center of 2.1×10^4 (adopting a total mass density

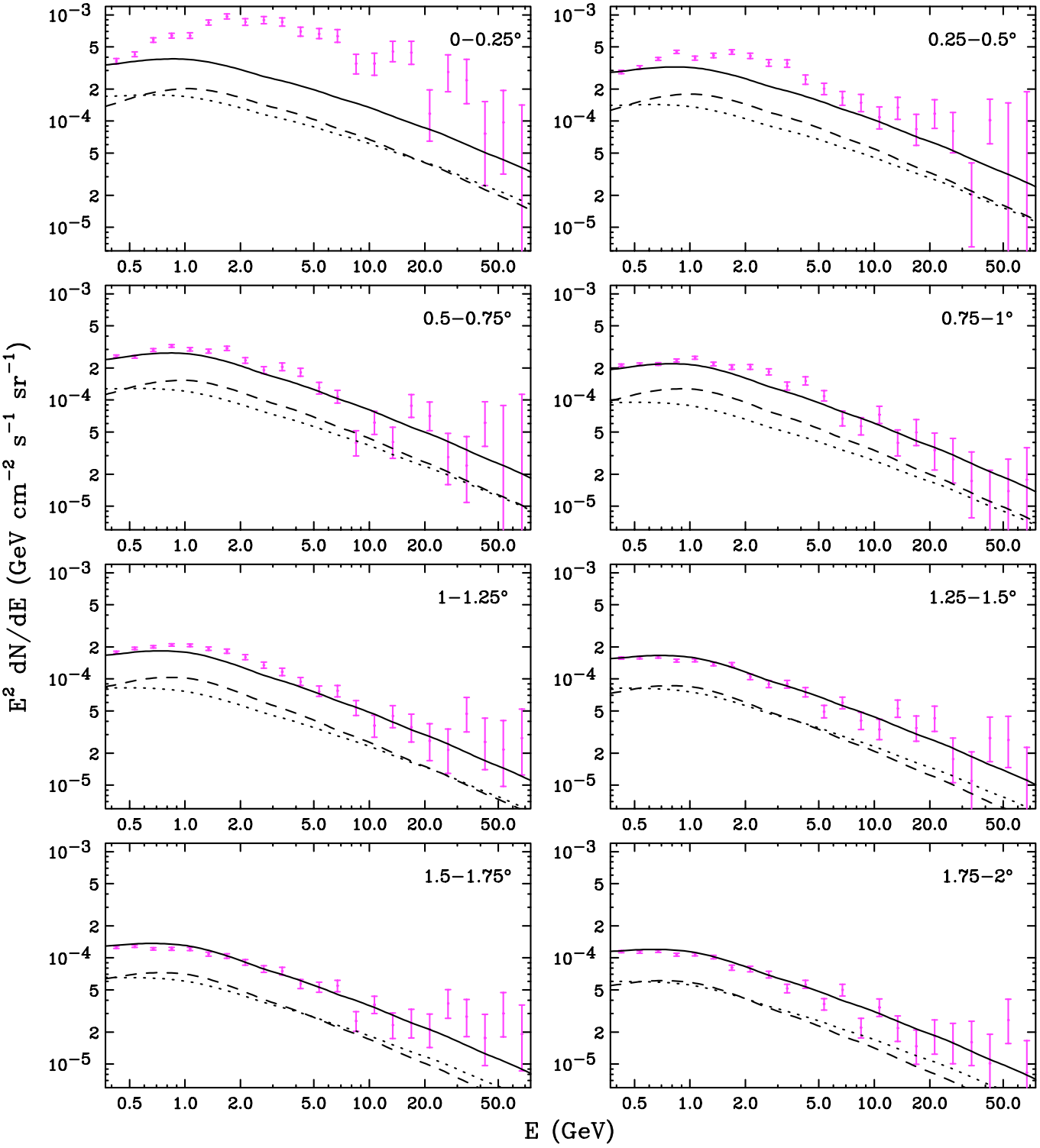

FIG. 11: The total observed gamma ray spectra in various ranges of the angular distance from the Galactic Center, compared to the bulge (dotted) and disk (dashed) components of our background model (the solid line denotes the sum of the bulge and disk components). Outside of 1.25° from the Galactic Center, this model describes the data very well. Closer to the Galactic Center, however, the spectral shape of the observed emission is significantly different, peaking at 1-5 GeV. See text for details.

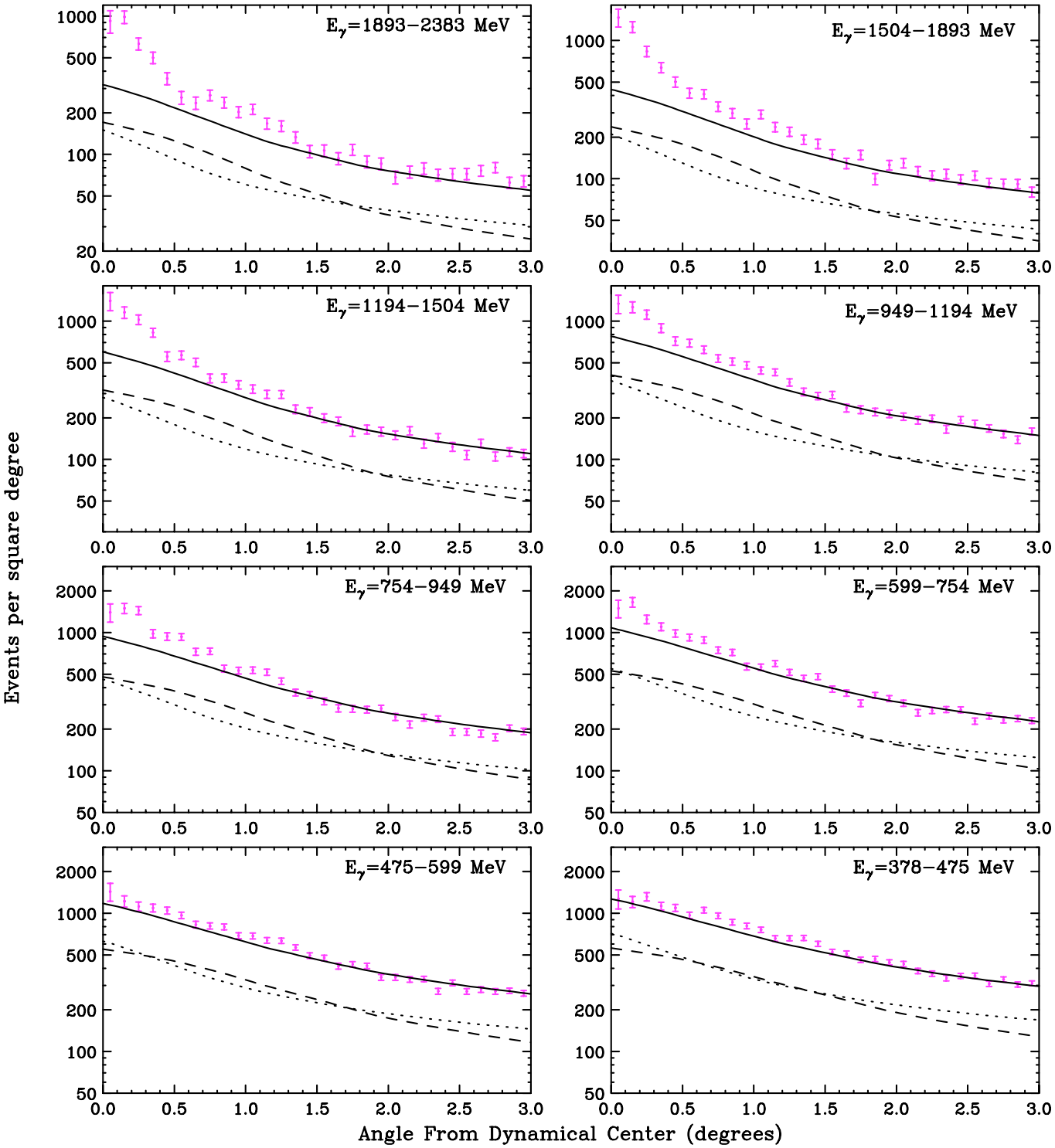

FIG. 12: The angular profile of the emission that is distributed with spherical symmetry around the Galactic Center. The bulge, disk and bulge+disk components are shown as dotted, dashed solid lines, respectively. An excess relative to these backgrouds is evident within 1.25° of the Galactic Center, between approximately 600 MeV and 6 GeV.

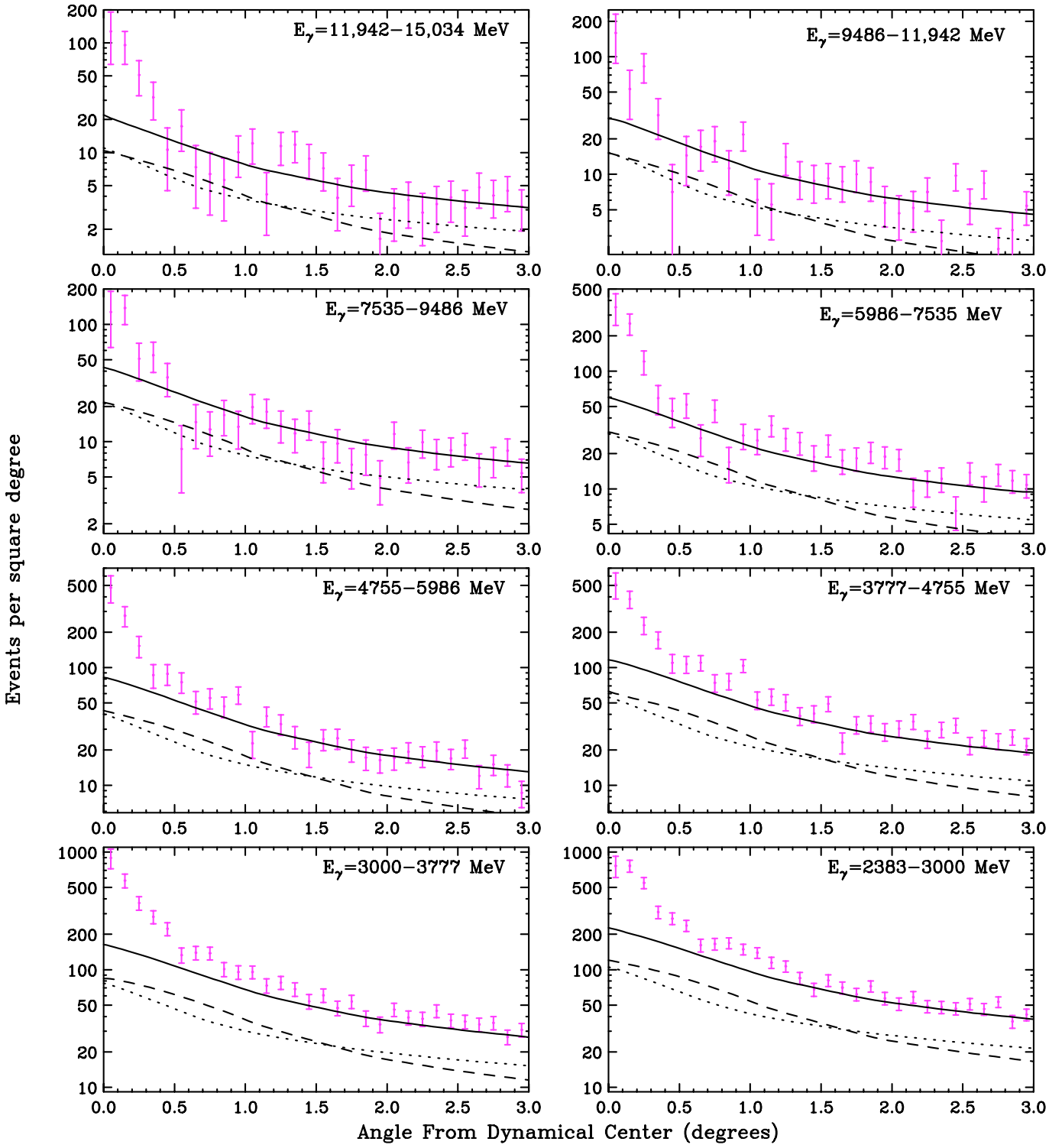

FIG. 13: The angular profile of the emission that is distributed with spherical symmetry around the Galactic Center. The bulge, disk and bulge+disk components are shown as dotted, dashed solid lines, respectively. An excess relative to these backgrouds is evident within 1.25° of the Galactic Center, between approximately 600 MeV and 6 GeV.

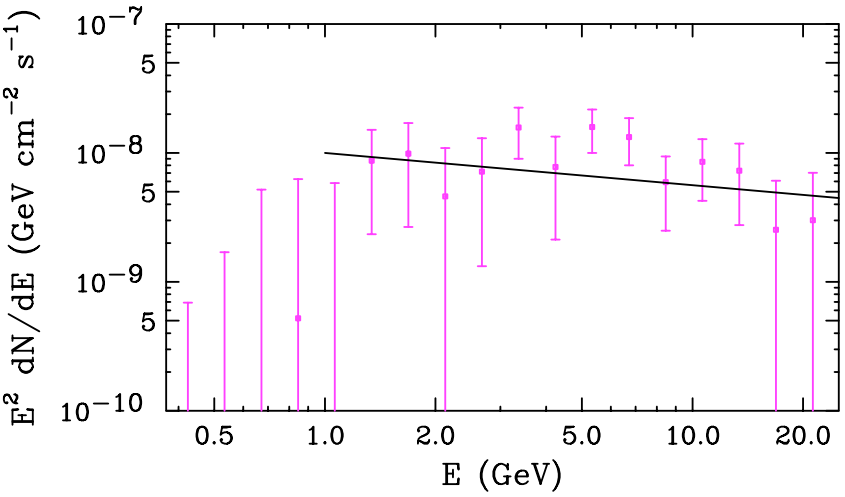

FIG. 14: The spectrum of the emission from the Galactic Center point source (likely associated with our Galaxy's supermassive black hole [17]). For comparison, we show the extrapolation of the power-law spectrum reported by HESS [12] and other ground based gamma ray telescopes [16]. The spectrum shown has been corrected to account for the finite point spread function of FGST.

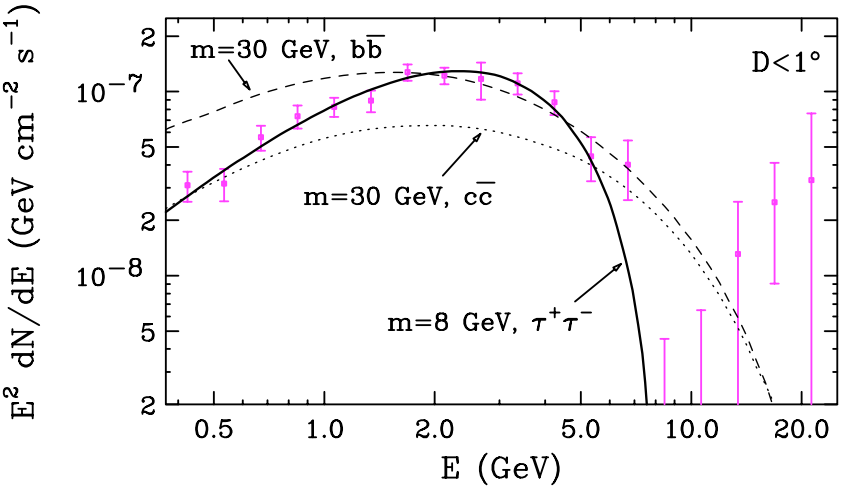

FIG. 15: The spectrum of the excess emission in the region within 1° of the Galaxy's dynamical center (by excess, we mean that emission not associated with the disk, bulge, or resolved point sources). The spectrum shown has been corrected to account for the finite point spread function of FGST. We also compare the observed spectrum with that predicted from annihilating dark matter (solid, dashed and dotted lines). The case of an approximately 8 GeV particle annihilating to tau leptons provides a particularly good fit to the data.

within the Solar Circle fixed to a that of an NFW profile with a local density of 0.3 GeV/cm^3). In contrast, if an NFW-like slope of $\gamma = 1$ is found outside of the innermost 500 pc of Galaxy, at which point the transition to a slope of 1.34 takes place, we find an averaged value of $J = 6.8 \times 10^3$. For the case of a dark matter particle with a mass of 8 GeV and that annihilates to $\tau^+\tau^-$ (as shown in Fig. 15), these profiles would imply values of $\langle \sigma v \rangle \approx 3.3 \times 10^{-27}$ cm^3/s and 1.5×10^{-26} cm^3/s, respectively. Of course, these values represent only the annihilation cross section to $\tau^+\tau^-$ and, if other annihilation channels that do not yield a large flux of gamma rays are significant, the total cross section may be larger.

VI. OTHER INTERPRETATIONS?

In this section, we discuss explainations other than dark matter annihilations that might account for the observed emission from the inner volume of the Milky Way. Both the spectral shape and angular distribution of the observed signal, however, are difficult to astrophysical sources or mechanisms. In particular, within the inner $\sim$0.25°, the additional (*ie.* non-pion, non-inverse Compton) component dominates over the other sources of 1-5 GeV gamma rays, but is entirely indiscernible beyond 1.25° from the Galactic Center. This requires the sources of the emission to be highly concentrated within a region only a few tens of parsecs in radius (recall that the best fit distribution of the sources of the excess emission is proportional to $r^{-2.68}$). Although one might imagine this excess emission to be the product of a large number of unresolved point sources with spectra that peak in the 2-4 GeV range (millisecond pulsars, for example), it is difficult to imagine why the number density of such sources would be almost 500 times greater 10 parsecs from the Galactic Center than at a distance of 100 parsecs. Even modest pulsar kicks of ~ 100 km/s would allow a pulsar 10 pc from the Galactic Center to escape the region, consequently broading the angular width of the signal. Annihilating dark matter, in contrast, produces a flux of gamma ray that scales with its density *squared*, and thus can much more easily account for the high concentration of the observed signal. Furthermore, based on observations of resolved millisecond pulsars in other regions by FGST, the average spectrum of such objects takes the form of $dN_\gamma/dE_\gamma \propto E_\gamma^{-1.5} \exp(-E_\gamma/2.8\,\mathrm{GeV})$ (as shown in the left frame of Fig. 16) [18], whereas the spectrum of the excess emission from the Inner Galaxy rises with a much harder spectral index, $dN_\gamma/dE_\gamma \propto E_\gamma^{-0.5} \exp(-E_\gamma/1.5\,\mathrm{GeV})$. Among the 46 gamma ray pulsars in the FGST's first pulsar catalog, none have exhibited a spectral index as hard as that required to accomodate the observed excess [19]. Unless the population of pulsars in the inner tens of parsecs of our galaxy produce a much harder gamma ray spectrum, on average, than those observed elsewhere, they cannot explain the observed excess.

Alternatively, one could consider the possibility that the excess emission originates from neutral pions produced in the collisions of cosmic rays with gas, but with a much harder spectrum than is found in other regions of the Galaxy. This, however, turns out to be implausible upon closer inspection. If we harden the cosmic ray proton spectrum, the gamma ray peak does shift to the right, but not with the rapid climb and sudden fall manifest in the spectrum shown in Fig. 15. To generate such a sharp peak at 2-3 GeV, one could consider a strongly broken power-law for the cosmic ray spectrum, but even this is unable to generate the observed gamma ray spectrum. In the right frame of Fig. 16, we show the gamma ray spectrum from pion decays (as calculated using GALPROP [15]) assuming an injected proton spectrum given by $dN_p/dE_p \propto E_p^{-0.5}$ below 50 GeV, and $dN_p/dE_p \propto E_p^{-5}$ above 50 GeV. Even this very extreme proton spectrum fails to generate the observed spectral peak. We thus conclude that the observed excess cannot be the accounted for by the decay of cosmic ray induced pions.

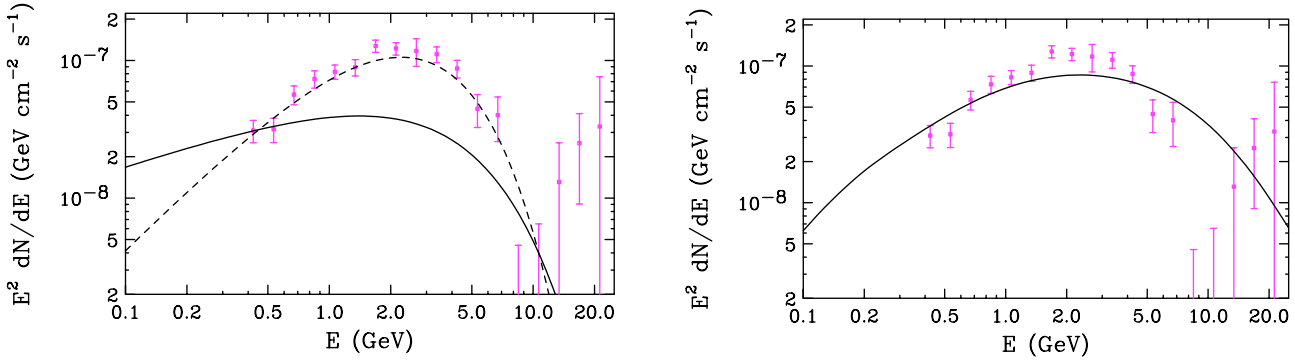

FIG. 16: Left: The spectrum of the excess emission compared to the average spectrum of observed millisecond pulsars, $dN_\gamma/dE_\gamma \propto E_\gamma^{-1.5} \exp(-E_\gamma/2.8\,\mathrm{GeV})$ (solid). The dashed curve, in contrast, represents the much harder spectrum, required to fit the observations, $dN_\gamma/dE_\gamma \propto E_\gamma^{-0.5} \exp(-E_\gamma/1.5\,\mathrm{GeV})$. Right: The spectrum of the excess emission compared to the spectrum from pion decay assuming a rather extreme (and implausible) cosmic ray proton spectrum of $dN_p/dE_p \propto E_p^{-0.5}$ and $dN_p/dE_p \propto E_p^{-5}$ below and above 50 GeV, respectively. Even this cannot generate the very steep 2-3 GeV peak that is observed.

Lastly, we note that if the point spread function of FGST were considerably less accurate than the values used in our study (and that are quoted by the FGST collaboration [14]), the bright point source at the Galaxy's dynamical center could plausibly account for the observed excess. In Fig. 17, we show the angular profile of the observed emission in a representative energy bin, showing results for the central point source (dotted line), the disk and bulge emission (dashed line), and the sum of all components, including the best-fit dark matter profile. From this figure, it is clear

that a point-like source cannot account for the observed profile of gamma rays. Only if the FGST's PSF were broader by a factor of ∼3 could the observed angular extent of the excess emission be accounted for in this way.

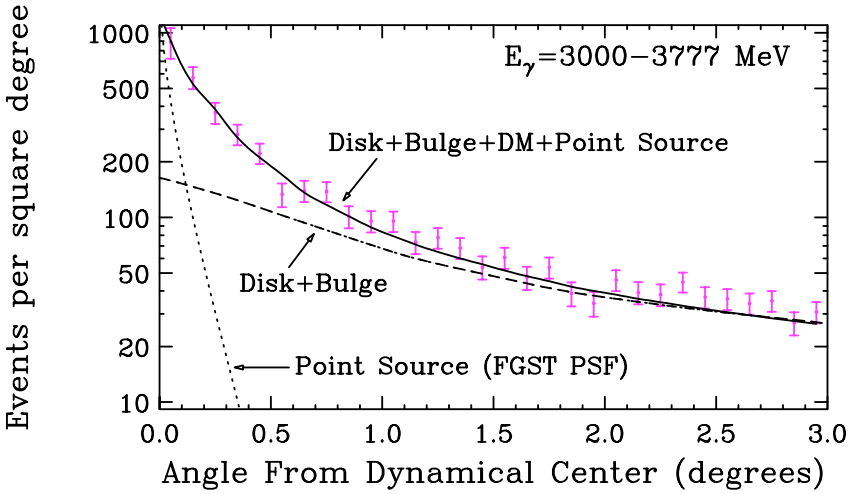

FIG. 17: The angular profile of the emission in a representative energy bin, as also shown in Fig. 13, compared to the predicted profiles for the emission from the central point source (dotted), the disk and bulge emission (dashed), and the sum of all components (solid), including the best-fit dark matter profile. A point-like source clearly cannot account for the observed emission.

VII. COMPARISONS WITH OUR PREVIOUS STUDY

In a previous paper [7], we analyzed the first year of FGST data from the inner 3° around the Galactic Center, and reached similar (although not identical) conclusions to those described here. In particular, both studies identified a bump-like feature peaking at 2-5 GeV in the inner degree or so of the Inner Galaxy. We will now briefly discuss the differences between the results presented in Ref. [7] and those presented here.

For this work, we modelled the backgrounds in a significantly more sophisticated way than was done in Ref. [7]. Although Ref. [7] used a background with a similar morphology to our disk-component, spherically symmetric, bulge-like backgrounds were not considered. As a result, the slope of the best fit halo profile was found to be somewhat shallower than those found here ($\gamma \approx 1.1$ rather than 1.34 ± 0.04). In other words, the excess component described in Ref. [7] consists of a combination of the excess component described in this paper and emission from pion decay (and inverse Compton scattering) in the bulge. As a consequence, the fits of Ref. [7] required a somewhat higher overall dark matter annihilation rate that that found here.

Furthermore, the spectral shape of the background used in Ref. [7] was fit to a power-law, and thus did not account for the details of the pion decay (plus inverse Compton scattering) spectrum that was shown in this paper to well describe the observed disk and bulge emission. This had the net effect of skewing the spectral shape of the extracted excess in the inner degree (compare Fig. 2 of Ref. [7] to Fig. 15 of this paper). The somewhat broader spectral feature found in Ref. [7] was shown to be adequately fit by a 25-30 GeV dark matter annihilating to $b\bar{b}$. This scenario, however, does not provide a good fit to the spectrum found here (see Fig. 15). Instead, we find good fits only for dark matter with a mass of 7.3-9.2 GeV, and that annihilates to tau leptons.

VIII. DISCUSSION AND CONCLUSIONS

In this paper, we analyzed the first two years of data from the Fermi Gamma Ray Space Telescope (FGST) with the intention of constraining or identifying the products of dark matter annihilations taking place in the inner volume of the Milky Way. We have identified a component of gamma ray emission concentrated within the inner degree of the Galactic Center (but that is not point-like in nature), with a spectrum peaking at 2-4 GeV (in E^2 units). This emission does not appear to be consistent with any known astrophysical backgrounds. In contrast, this signal can easily be accounted for by annihilating dark matter. In particular, the observed morphology and spectrum of the

signal can be well fit by dark mater distributed in a profile described by $\rho \propto r^{-1.34\pm0.04}$, with a mass of 7.3 to 9.2 GeV, and that annihilates primarily to tau leptons (see Fig. 15). Depending on how the dark matter distribution is normalized, the required annihilation cross section falls within the range of $\langle \sigma v \rangle = 3.3 \times 10^{-27}$ to 1.5×10^{-26} cm^3/s.

The characteristics of the dark matter implied by these observations are consistent with theoretical expectations. In particular, the required dark matter distribution is in concordance with that predicted by numerical simulations [8], after accounting for a moderate degree of adiabatic contraction [9]. Furthermore, the annihilation cross section required to normalize the signal is approximately equal to that of a simple thermal relic that freezes out with an abundance equal to the measured cosmological density of dark matter. Furthermore, we point out that the dark matter mass implied by this observation is remarkably similar to that needed to simultaneously explain the observations by the direct detection experiments CoGeNT [20] and DAMA [21]. In particular, it was shown in Ref. [22] that the signals reported by the CoGeNT and DAMA collaborations can be consistently interpreted as elastically scattering dark matter particles with masses in the range of approximately 6.2 to 8.6 GeV (see also Ref. [23]).

In the dark matter scenario implied by the observations described in this paper, gamma rays are not the only potentially observable annihilation products. In particular, the electrons produced in the annihilations of dark matter (through either subsequent tau decays, or through annihilations directly to e^+e^- and/or $\mu^+\mu^-$) will produce synchrotron emission peaking at frequences of $\nu_{\rm syn} \sim 23$ GHz $\times$ $(E_e/7$ GeV$)^2$ $(B/100\,\mu$G). Given the recently reported evidence of 100 microGauss-scale magnetic fields in the Inner Galaxy [24], it is not difficult to interpret the so-called WMAP haze [25] as a signal of the dark matter particle described in this paper.

Acknowledgments

We would like to thank Greg Dobler for providing the curves presented in Fig. 9. We would also like to thank Doug Finkbeiner, Tim Linden, Patrick Fox, Scott Dodelson, Kathryn Zurek, and Joachim Kopp for helpful discussions and comments. This work has been supported by the US Department of Energy and by NASA grant NAG5-10842. Fermilab is operated by Fermi Research Alliance, LLC under Contract No. DE-AC02-07CH11359 with the United States Department of Energy.

[1] L. Bergstrom, P. Ullio and J. H. Buckley, Astropart. Phys. **9**, 137 (1998) [arXiv:astro-ph/9712318]; V. Berezinsky, A. Bottino and G. Mignola, Phys. Lett. B **325**, 136 (1994) [arXiv:hep-ph/9402215].

[2] A. A. Abdo, M. Ackermann, M. Ajello *et al.*, Astrophys. J. **712**, 147-158 (2010). [arXiv:1001.4531 [astro-ph.CO]]; P. Scott, J. Conrad, J. Edsjo *et al.*, JCAP **1001**, 031 (2010). [arXiv:0909.3300 [astro-ph.CO]].

[3] M. Ackermann, M. Ajello, A. Allafort *et al.*, JCAP **1005**, 025 (2010). [arXiv:1002.2239 [astro-ph.CO]]; L. Dugger, T. E. Jeltema, S. Profumo, [arXiv:1009.5988 [astro-ph.HE]].

[4] A. A. Abdo *et al.* [Fermi-LAT Collaboration], JCAP **1004**, 014 (2010). [arXiv:1002.4415 [astro-ph.CO]].

[5] A. A. Abdo *et al.* [Fermi LAT Collaboration], Phys. Rev. Lett. **103**, 251101 (2009). [arXiv:0912.0973 [astro-ph.HE]]; T. A. Porter, f. t. F. L. Collaboration, [arXiv:0907.0294 [astro-ph.HE]].

[6] M. R. Buckley, D. Hooper, Phys. Rev. **D82**, 063501 (2010). [arXiv:1004.1644 [hep-ph]].

[7] L. Goodenough, D. Hooper, [arXiv:0910.2998 [hep-ph]].

[8] J. F. Navarro, C. S. Frenk and S. D. M. White, Astrophys. J. **462**, 563 (1996) [arXiv:astro-ph/9508025]; J. F. Navarro, C. S. Frenk and S. D. M. White, Astrophys. J. **490**, 493 (1997).

[9] O. Y. Gnedin, A. V. Kravtsov, A. A. Klypin and D. Nagai, Astrophys. J. **616**, 16 (2004) [arXiv:astro-ph/0406247]; F. Prada, A. Klypin, J. Flix, M. Martinez and E. Simonneau, arXiv:astro-ph/0401512; G. Bertone and D. Merritt, Mod. Phys. Lett. A **20**, 1021 (2005) [arXiv:astro-ph/0504422]; G. Bertone and D. Merritt, Phys. Rev. D **72**, 103502 (2005) [arXiv:astro-ph/0501555]; Y. Mambrini, C. Munoz, E. Nezri and F. Prada, JCAP **0601**, 010 (2006) [arXiv:hep-ph/0506204]; R. Levine, N. Y. Gnedin, A. J. S. Hamilton and A. V. Kravtsov, Astrophys. J. **678**, 154 (2008) [arXiv:0711.3478 [astro-ph]].

[10] E. Komatsu *et al.* [WMAP Collaboration], Astrophys. J. Suppl. **180**, 330-376 (2009). [arXiv:0803.0547 [astro-ph]].

[11] S. Dodelson, D. Hooper and P. D. Serpico, Phys. Rev. D **77**, 063512 (2008) [arXiv:0711.4621 [astro-ph]]; G. Zaharijas and D. Hooper, Phys. Rev. D **73**, 103501 (2006). [arXiv:astro-ph/0603540]; D. Hooper and B. L. Dingus, Phys. Rev. D **70**, 113007 (2004) [arXiv:astro-ph/0210617].

[12] F. Aharonian *et al.* [The HESS Collaboration], F. Aharonian *et al.* [The HESS Collaboration], Astron. Astrophys. **425**, L13-L17 (2004). [astro-ph/0408145]; C. van Eldik *et al.* [HESS Collaboration], J. Phys. Conf. Ser. **110**, 062003 (2008). [arXiv:0709.3729 [astro-ph]].

[13] The Fermi-LAT Collaboration, Astrophys. J. Suppl. **188**, 405 (2010) [arXiv:1002.2280 [astro-ph.HE]].

[14] `http://www-glast.slac.stanford.edu/software/IS/glast_lat_performance.htm`

[15] A. W. Strong, I. V. Moskalenko, T. A. Porter *et al.*, [arXiv:0907.0559 [astro-ph.HE]].

[16] K. Kosack *et al.* [The VERITAS Collaboration], Astrophys. J. **608**, L97 (2004) [arXiv:astro-ph/0403422]; J. Albert *et al.* [MAGIC Collaboration], Astrophys. J. **638**, L101 (2006) [arXiv:astro-ph/0512469].
[17] F. Aharonian and A. Neronov, Astrophys. J. **619**, 306 (2005) [arXiv:astro-ph/0408303]; arXiv:astro-ph/0503354; AIP Conf. Proc. **745**, 409 (2005); A. Atoyan and C. D. Dermer, Astrophys. J. **617**, L123 (2004) [arXiv:astro-ph/0410243].
[18] A. A. Abdo *et al.* [Fermi-LAT Collaboration], Science, 325 848 (2009); D. Malyshev, I. Cholis, J. D. Gelfand, [arXiv:1002.0587 [astro-ph.HE]].
[19] A. A. Abdo *et al.* [Fermi LAT Collaboration], Astrophys. J. Suppl. **187**, 460-494 (2010). [arXiv:0910.1608 [astro-ph.HE]].
[20] C. E. Aalseth *et al.* [CoGeNT Collaboration], [arXiv:1002.4703 [astro-ph.CO]].
[21] R. Bernabei, P. Belli, F. Cappella *et al.*, Eur. Phys. J. **C67**, 39-49 (2010). [arXiv:1002.1028 [astro-ph.GA]].
[22] D. Hooper, J. I. Collar, J. Hall *et al.*, Phys. Rev. D, in press, [arXiv:1007.1005 [hep-ph]].
[23] A. L. Fitzpatrick, D. Hooper, K. M. Zurek, Phys. Rev. **D81**, 115005 (2010). [arXiv:1003.0014 [hep-ph]]; A. V. Belikov, J. F. Gunion, D. Hooper *et al.*, [arXiv:1009.0549 [hep-ph]]; S. Chang, J. Liu, A. Pierce *et al.*, JCAP **1008**, 018 (2010). [arXiv:1004.0697 [hep-ph]]; S. Andreas, C. Arina, T. Hambye *et al.*, Phys. Rev. **D82**, 043522 (2010). [arXiv:1003.2595 [hep-ph]].
[24] R. Crocker *et al.*, Nature 463, 65-67 (2010).
[25] D. Hooper, D. P. Finkbeiner and G. Dobler, Phys. Rev. D **76**, 083012 (2007) [arXiv:0705.3655 [astro-ph]]; D. P. Finkbeiner, arXiv:astro-ph/0409027; D. Hooper, G. Zaharijas, D. P. Finkbeiner, and G. Dobler, Phys. Rev. D **77**, 043511 (2008) [arXiv:0709.3114 [astro-ph]].